Effects of Additive and Preheat on the Partially Premixed CH_4-Air Counter Flow Flames Considering Non-gray Gas Radiation

Won-Hee Park
Track & Civil Engineering Research Department,
Korea Railroad Research Institute 437-757, Korea
Hee-Chul Chang
Graduate School Chung-Ang University, Seoul 156-756, Korea
Tae-Kuk Kim*
Department of Mechanical Engineering, Chung-Ang University, Seoul, 156-756, Korea

Detailed structures of the counterflow flames formed for different inlet fluid temperatures and different amount of additives are studied numerically. The detailed chemical reactions are modeled by using the CHEMKIN-II code. The discrete ordinates method and the narrow band based WSGGM with a gray gas regrouping technique (WSGGM-RG) are applied for modeling the radiative transfer through non-homogeneous and non-isothermal combustion gas mixtures generated by the counterflow flames. The results compared with those obtained by using the SNB model show that the WSGGM-RG is very successful in modeling the counterflow flames with non-gray gas mixture. The numerical results also show that the addition of CO_2 or H_2O to the oxidant lowers the peak temperature and the NO concentration in flame. But preheat of fuel or oxidant raises the flame temperature and the NO production rates. O_2 enrichment also causes to raise the temperature distribution and the NO production in flame. And it is found that the O_2 enrichment and the fuel preheat were the major parameters in affecting the flame width.

Key Words: Radiative Heat Transfer, Counterflow Flame, Combustion, Laminar Flow, WSGGM-RG, Discrete Ordinates Method

1. Introduction

The counterflow combustion system has been often considered in many studies. It has some advantages in both experimental and numerical studies due to its simplicity, since the counterflow combustion system can be approximated as an axisymmetric flow system with nearly one-dimensional heat flow. And the flow field computation could be easy by considering laminar flow. Therefore the laminar counterflow combustion system is very useful and powerful to observe the effects of inlet velocity, temperature changes, concentration, additives, radiative heat transfer and others. Study on laminar flame is not only profitable itself but also significant for turbulent combustion studies.

There have been many different studies on the effects of additives such as CO_2 for more than 40 years (McLintock, 1968). Du et al.(1991) concluded that the introduction of additives generally affects soot formation through the following three ways ; dilution effect, thermal effect and the direct chemical effect. Liu et al.(2001) investigated the mechanism of the chemical effects of CO_2 addition on soot and NO_X formation in a counterflow diffusion flame. Li et al.(1999) studied the influences of staging and diluent addition. They identified important reactions for pollutant for-

* Corresponding Author,
E-mail : kimtk@cau.ac.kr
TEL : +82-2-820-5282; **FAX** : +82-2-814-9476
Energy System Laboratory, School of Mechanical Engineering, Chung-Ang University, 221, Huksuk-Dong, Dongjak-Ku, Seoul 156-756, Korea. (Manuscript **Received** June 28, 2005; **Revised** December 21, 2005)

mation and suggested means to reduce emissions by verifying through the measurement and numerical computations.

Radiative heat transfer has often been neglected in combustion modeling, but recent works considering radiative heat transfer lead to more improved results. Zhu et al.(2003) studied self-absorption effects of radiation for a counterflow partially premixed flame. The results show that self-absorption must be considered for modeling a relatively thick double flame structure and a reaction zone that is sensitive. And comparing the results of experiments and computations, they showed that the mechanism of GRI-MECH 2.11 (http//www.me.berkeley.edu/grimech) yields better agreements with the experimental data than the GRI-MECH 3.0 mechanism (Zhu et al., 2002). Kim et al.(2003) applied a WSGGM-based low-resolution spectral model for the radiation properties of combustion gases. It is developed using a narrow-band model to estimate self-absorption of radiation in one-dimensional counterflow diffusion flames. It shows that the model coupled to the OPPDIF code (Lutz et al., 1997) predicts the self-absorption of radiation energy very well compared with the results of the statistical narrow-band model. Guo et al.(1998) investigated the effects of radiative heat loss and extinction characteristics. $CH_4/CO_2/Air$ and $CH_4/CO_2/O_2$ counterflow premixed systems were considered and analyzed numerically using the detailed chemistry and transport properties with emphasis on assessing the importance of radiation reabsorption. It is also important to study the effects of inlet temperature changes on gas mixtures. Lim et al.(2000) investigated the effects of air preheat on flame structure in CH_4/Air counterflow diffusion flames using experimental and numerical methods. Lee (2004) investigated the change in the NO emission indices due to the interaction between a vortex and methane-air flames.

The purpose of the present article is to investigate the effects of the inlet temperature changes of gases and the introduction of additives such as CO_2 or H_2O by considering the radiative heat loss. Calculations were performed using the OPPDIF code developed in Sandia National Laboratory. GRI-MECH 2.11 mechanism containing 279 elementary reactions and involving 49 chemical species was considered (http://www.me.berkeley.edu/grimech). Chemkin-II database was used to obtain the necessary thermochemical and transport properties (Kee et al., 1989). And radiative heat transfer computation was performed by using the discrete ordinates method with the WSGGM regrouping technique (Park and Kim, 2003; 2005).

2. Theory

2.1 Counterflow combustion system

The counterflow combustion system considered here is illustrated in Fig. 1. Air or Air with additive is ejected from the lower nozzle and fuel or fuel with air is ejected from the upper nozzle. Therefore the stagnation plane occurs between the upper and the lower nozzles. The premixed flame near the fuel nozzle is observed to be green while the diffusion flame is blue (Li et al., 1999). Assuming that the flow is laminar and axisymmetric then we can easily observe the effects according to the changes of temperature, concentration, velocity etc. Due to its simplicity the counterflow combustion system has been considered in many experimental and numerical studies.

2.2 Governing equations

To analyze the counterflow combustion system several equations can be derived by using the coordinate system shown in Fig. 1. Mass conservation equation using the cylindrical coordinate

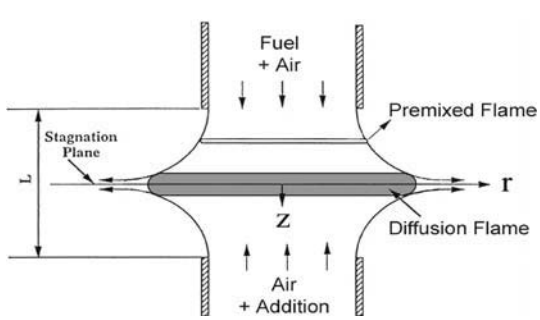

Fig. 1 Schematic diagram of the system

at steady state can be written as

$$\frac{\partial}{\partial x}(\rho u)+\frac{1}{r}\frac{\partial}{\partial r}(\rho v r)=0 \tag{1}$$

where u and v are axial and radial velocity components respectively. ρ is the mass density of gas mixture. According to the assumption that all the quantities including radial velocity and temperature etc. are functions of x only, conservation equation can be simplified as

$$\frac{dJ}{dx}-G=0 \tag{2}$$

where $J=\rho u/2$ and $G=-\rho v/r$ are axial and radial mass flux components respectively. Radial momentum equation can be written as

$$H-2\frac{d}{dx}\left(\frac{JG}{\rho}\right)+\frac{3G^2}{\rho}+\frac{d}{dx}\left[\mu\frac{d}{dx}\left(\frac{G}{\rho}\right)\right]=0 \tag{3}$$

where μ is the fluid viscosity and H is given as $H=(1/\rho)(\partial p/\partial r)$. Energy conservation equation can be written as

$$\rho u\frac{dT}{dx}-\frac{1}{c_p}\frac{d}{dx}\left(\lambda\frac{dT}{dx}\right)+\frac{\rho}{c_p}\sum_k c_{pk}Y_kV_k\frac{dT}{dx}\frac{1}{c_p}\sum_k h_k\dot{w}_k+\frac{\nabla\cdot q}{c_p}=0 \tag{4}$$

where T, C_P, λ are temperature, specific heat capacity of gas mixture at constant pressure, and thermal conductivity respectively. $-\nabla\cdot q$ is the radiative heat source term. C_{pk}, Y_k, h_k, $\dot{\omega}_k$ represent specific heat capacity at constant pressure, mass fraction, enthalpy generation and chemical species generation rate of k-th species respectively. The conservation equation of chemical species can be expressed as

$$\rho u\frac{dY_k}{dx}-\frac{d}{dx}(\rho Y_kV_k)-\dot{\omega}_kW_k=0,\quad k=1,\ K \tag{5}$$

where W_k is the molecular weight of the k-th species. V_k represents the diffusion velocity of the k-th species and is written as

$$V_k=\frac{1}{X_k\bar{W}}\sum_{j=1}^{K}W_jD_{kj}\frac{dX_j}{dx}-\frac{D_k^T}{\rho Y_k}\frac{1}{T}\frac{dT}{dx} \tag{6}$$

where D_{kj}, D_k^T, X_k are the multicomponent mass diffusion coefficient, thermal diffusion coefficient, mole fraction of k-th species respectively. And the equation of state is given by

$$p=\frac{\rho RT}{\bar{W}} \tag{7}$$

where $\bar{W}$ is the mean molecular weight of gas mixture. The boundary conditions for each nozzles are

$$x=0:\ F=\frac{\rho_F u_F}{2},\ G=0,\ T=T_F,\quad \rho uY_k+\rho Y_kV_k=(\rho uY_k)_F \tag{8}$$

$$x=L:\ F=\frac{\rho_0 u_0}{2},\ G=0,\ T=T_0,\quad \rho uY_k+\rho Y_kV_k=(\rho uY_k)_0 \tag{9}$$

2.3 WSGGM with gray gas regrouping (WSGGM-RG)

In this study it is assumed that only CO_2 and H_2O gases participate by absorbing the radiative energy while all other gases are assumed to be transparent. The hypothesis that the spectra of the absorbing gases in a narrow band are not correlated is well known and holds for CO_2/H_2O gas mixture with fairly good accuracy (Goody et al., 1989 ; Lacis et al., 1991). Then the transmissivity of the gas mixture of CO_2 and H_2O over a narrow band can be obtained by multiplying the transmissivity of each gas (Modest, 1993) as

$$\bar{\tau}_{\eta,\mathrm{mix}}=\bar{\tau}_{\eta,\mathrm{CO_2}}\cdot\bar{\tau}_{\eta,\mathrm{H_2O}} \tag{10}$$

Therefore the average narrow band transmissivity of CO_2/H_2O mixture in the form of the narrow band based WSGGM (Kim et al., 1996 ; 2000) can be written as

$$\bar{\tau}_{\eta,\mathrm{mix}}=\sum_{i=1}^{M_{\mathrm{mix}}}W_{i,\mathrm{mix}}(\eta)\,e^{-\kappa_{i,\mathrm{mix}}L} \tag{11a}$$

or considering Eq. (10)

$$\tau_{\eta,\mathrm{mix}}=\sum_{ic=1}^{M_{\mathrm{CO_2}}}\sum_{ih=1}^{M_{\mathrm{H_2O}}}W_{ic,\mathrm{CO_2}}(\eta)\times W_{ih,\mathrm{H_2O}}(\eta)\,e^{-(\kappa_{ic,\mathrm{CO_2}}+\kappa_{ih,\mathrm{H_2O}})L} \tag{11b}$$

By comparing Eq. (11a) with (11b), the spectral weighting factor $W_{\mathrm{mix}}(\eta)$ and the absorption coefficient $\kappa_{i,\mathrm{mix}}$ for the gas mixture can be written as

$$W_{\mathrm{mix}}(\eta)=W_{\mathrm{CO_2}}(\eta)\times W_{\mathrm{H_2O}}(\eta) \tag{12a}$$

$$\kappa_{i,\mathrm{mix}}=\kappa_{i,\mathrm{CO_2}}+\kappa_{i,\mathrm{H_2O}} \tag{12b}$$

The number of gray gases replacing the real gas mixture, M_{mix}, is M^2 when $M=M_{\mathrm{CO_2}}=M_{\mathrm{H_2O}}$. Using the absorption coefficient suggested by

Kim and Song (2000), the local gray gas absorption coefficient of CO_2/H_2O mixture can be written as

$$\kappa_{i,\mathrm{mix}}=\kappa_{i0,\mathrm{CO_2}}\frac{e^{-\alpha_{i,\mathrm{CO_2}}/T}}{T^2}pX_{\mathrm{CO_2}}+\kappa_{i0,\mathrm{H_2O}}\frac{e^{-\alpha_{i,\mathrm{H_2O}}/T}}{T^2}pX_{\mathrm{H_2O}} \quad (13)$$

Since the number of gray gases required for replacing the real gas mixtures is very large (when $M=30$, $M^2=900$ gray gases), a gray gas regrouping process which enables us to reduce the number of gray gases to a designated number is introduced in order to improve the computational efficiency of the WSGGM for gas mixtures while the accuracy of the WSGGM is reserved (Park et al., 2003 ; 2005). The gray gas regrouping process is performed comparing the magnitudes of the gray gas absorption coefficients for the reference state. The new weighting factor, $W_{i,\mathrm{new}}$ is obtained by simply summing up the original weighting factors of the gray gases in the i-th group as

$$W_{i,\mathrm{new}}(\eta)=\sum_{j=1}^{N_i} W_{j,\mathrm{mix}}(\eta) \quad (14)$$

where N_i is the number of gray gases in the i-th group and the subscript 'new' means the parameter after the gray gas regrouping process.

The new absorption coefficient for the i-th group, $\kappa_{i,\mathrm{new}}$, can be obtained by using the Planck mean type absorption coefficient and written as

$$\kappa_{i,\mathrm{new}}=\frac{\sum_{j=1}^{N_i}\kappa_{j,\mathrm{mix}}W_{j,\mathrm{mix}}}{W_{i,\mathrm{new}}} \quad (15)$$

where the total weighting factor for the i-th group can be given by using the spectral weighting factors of the i-th group.

$$W_{i,\mathrm{new}}=\frac{\sum_{\eta} W_{i,\mathrm{new}}(\eta)\,I_b(\eta)\Delta\eta}{\sum_{\eta} I_b(\eta)\Delta\eta} \quad (16)$$

Physically the weighting factor in Eq. (16) corresponds to the blackbody energy fraction in the spectral region of the effective absorption coefficient.

2.4 Radiative transfer

Assuming one-dimensional infinite plate of length L filled with real gases, radiative intensity at point p and in the direction of m can be written by using the discrete ordinate method (Kim et al., 1991) as

$$I_{i,p,m}=\frac{\mu_m I_{i,w,m}+fW_{i,p}\kappa_{i,p}I_{b,p}\Delta x_p}{\mu_m+fW_{i,p}\kappa_{i,p}\Delta x_p} \quad (17)$$

where subscripts i, p and m represent the i-th gray gas, position and direction respectively. μ_m is the directional cosine of m-th direction. f is the weighting factor for calculating the intensity, $I_{i,e,m}$, at the east face of the control volume. Then $I_{i,p,m}$ can be determined by using the weighting factor, f as

$$I_{i,p,m}=fI_{i,e,m}+(1-f)\,I_{i,w,m} \quad (18)$$

Finally the radiative heat source term at point 'p' can be calculated as

$$-\nabla\cdot q_p=-\left[\sum_{m=1}^{N_q}\mu_m(I_{e,m}-I_{w,m})\,w_m\right]/\Delta x_p \quad (19)$$

where ω_m is the angular weighting factor for m-th direction and N_q is the number of total angular directions considered. For the SNB model, the spectral data of Soufiani and Taine (1997) were used. And the one dimensional code (Kim et al., 1991) is modified to analyze the radiative heat transfer equations with the WSGG-RG model.

3. Numerical Results and Discussion

In this work detailed structures of the laminar counterflow flames formed for different inlet temperatures and for different additives are studied numerically considering radiative heat transfer. Distance between the fuel and the oxidant nozzles is 2 cm and the total pressure is 1 atm. Methane and air were used as fuel and oxidant. GRI-MECH 2.11 contains 279 chemical reactions and involves 49 species while GRI-MECH 3.0 includes 325 chemical reactions and 53 species. Since the results using GRI-MECH 2.11 yields better agreements with the results from experiments than GRI-MECH 3.0, GRI-2.11 is considered in this study. Chemkin-II database is used to get the necessary thermochemical and transport properties (Kee, 1989). And for the nongray radiative mixture gas, properties are modeled by using the WSGGM with gray gas regrouping (Park et al., 2003 ; 2005). S_{10} gaussian quadrature

Table 1 Operating condition for each flame

	Flame I	Flame II	Flame III	Flame IV	Flame V	Flame VI
V_F, V_o[cm/s]	10					
Gap between nozzles [cm]	2					
T_F[K]	300					300,400,500
T_O[K]	300				300,400,500	300
p_{total} [atm]	1					
ϕ	2					
Fuel Composition	CH_4/Air					
Oxidant Composition	Air	Air+CO_2	Air+H_2O	O_2+N_2	Air	Air

set is used for one-dimensional radiative analysis by using the discrete ordinates method. And it is assumed that only H_2O and CO_2 affects the radiative heat transfer. The assumed conditions for each combustion modeling are listed in Table 1.

3.1 Results for different radiative models (Flame I)

In this chapter the results obtained by using the "No Radiation" model (neglected radiation), the SNB model (reference data) and the WSGGM-RG (current) are compared with each other. For Flame I, the equivalence ratio, ϕ, is 2 and the inlet fluid velocities through each nozzles are 10 cm/s at 300K. Figure. 2 shows that the "No Radiation" model overestimates the peak temperature up to 4.4% as compared to the more accurate SNB model because it neglects the radiation effects. The current WSGGM-RG compares fairly well with the accurate SNB model. And the peak temperature of 1965K by the WSGGM-RG shows 0.76% relative error as compared to the SNB result (1980K). However the SNB model required 1982 seconds to complete the computation while the WSGGM-RG required only 103 seconds on the same pentium 4 2.6 GHz computer. Therefore we conclude that the WSGGM-RG is an effective and fairly accurate method and we will use the WSGGM-RG for the rest of our studies.

3.2 Effects by additives

3.2.1 Effects by CO_2 addition (Flame II)

It is known that the introduction of additives causes to change the flame structure significantly (McLintok, 1968; Du et al., 1991; Liu et al., 2001). CO_2 addition to the combustion zone appears in many practical combustion systems such as EGR (Exhaust Gas Recirculation). In

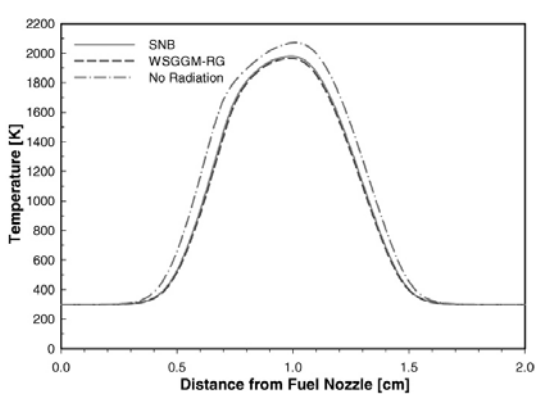

Fig. 2 Flame structure obtained for Flame I

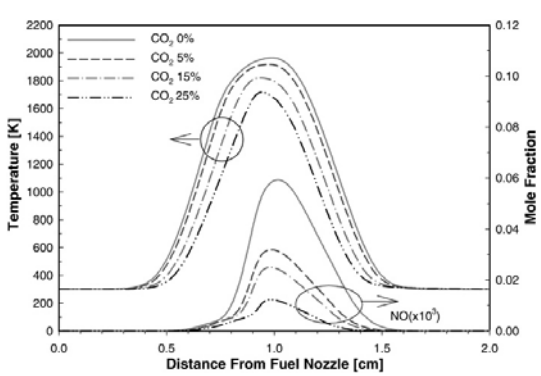

Fig. 3 Flame structure obtained for Flame II

this study the CO_2 addition rates (Flame II in Table 1) are considered from 0% to 25% with 5% increment by mole fraction and the corresponding amount of CO_2 is added to the oxidant nozzle. Inlet temperatures and velocities for both fuel and oxidant nozzles are set equal to 10 cm/s and 300K respectively. When 5% of CO_2 is introduced to the oxidant nozzle, the WSGGM-RG estimated the peak temperature to be 1918K which is 47K lower as compared to the result by no addition of CO_2. The peak NO mole fraction is estimated as 4.389×10^{-5} at 5% CO_2 addition which is 1.545×10^{-5} lower as compared to the result by no CO_2 addition. As the CO_2 concentration is increased to 25% the peak temperature and the peak NO mole fraction are estimated as 1718K and 1.232×10^{-5} respectively. For the same CO_2 concentration of 25% the WSGGM-RG estimates the peak temperature to be about 100K lower than the No radiation model. Such difference is due to the radiative heat loss from the dense CO_2 gas volume near the flame (Li et al., 1999).

3.2.2 Effects by H_2O addition (Flame III)

Addition of H_2O into the air nozzle causes similar effects on flame as the CO_2 addition. The operating condition shown in Table 1 is applied for the Flame III. The H_2O addition rates are considered from 0% to 25% with 5% increment by mole fraction. The inlet fluid temperatures and velocities of both sides are 300K and 10 cm/s respectively. When 5% of H_2O is added to the oxidant the peak temperature is estimated as 1938K which is 27K lower than that of no H_2O addition. The peak NO mole fraction is estimated as 4.500×10^{-5} at 5% H_2O addition which is 1.434×10^{-5} lower than that of no H_2O addition. As the H_2O concentration is increased to 25% the peak temperature and the peak NO mole fraction are estimated as 1793K and 1.247×10^{-5} respectively. For the same ranges of the H_2O concentration the WSGGM-RG results in the peak temperatures 90K-100K lower than those of the No radiation model. Our study shows that both CO_2 and H_2O additions to the oxidant show similar effects on flame temperature and NO generation.

3.2.3 Effects by O_2 enrichment (Flame IV)

The effect of the O_2 enrichment on the flame structure is studied by supplying the O_2+N_2 mixture at a designated volume fraction to the oxidant nozzle. And the mixture ratios of O_2 and N_2 are 9:1, 1:1 and 1:3.76 (standard air) by volume. Figure 5 shows that the peak flame temperature is

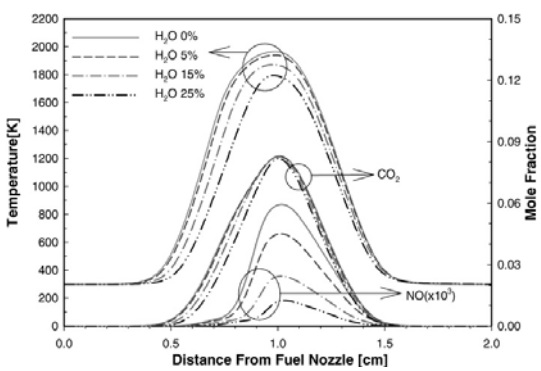

Fig. 4 Flame Structure obtained for Flame III

Table 2 Results for CO_2 addition

	CO_2 0%	CO_2 5%	CO_2 15%	CO_2 25%
Peak Temperature (K)	1965	1918	1820	1718
Peak NO mole fraction ($\times10^3$)	0.05934	0.04389	0.02497	0.01232

Table 3 Results for H_2O addition

	H_2O 0%	H_2O 5%	H_2O 15%	H_2O 25%
Peak temperature (K)	1965	1938	1869	1793
Peak NO mole fraction ($\times10^3$)	0.05934	0.0450	0.02431	0.01247
Peak CO_2 mole fraction	0.083	0.0829	0.0826	0.0817

increased as the O_2 concentration is increased. As the concentration of O_2 is increased from 50% to 90% the peak temperature is increased by 137K and the flame front is shifted to the fuel nozzle. And it is found that the O_2 enrichment causes to thicken the flame width.

3.3 Effects by preheat

In this study the effects by preheat of oxidant or fuel are studied numerically. The preheat of oxidant or fuel may affect the chemical reaction near the flame zone by activating some reactions or by suppressing some other reactions.

3.3.1 Effect by oxidant preheat (Flame V)

The effect by preheat of oxidant is studied by considering three different oxidant temperatures of T_O=300K, T_O=400K and T_O=500K. Figure 6 and Table 5 show that the preheat of oxidant from 300K to 500K causes to increase the peak flame temperature by 43K and the diffusion flame is shifted to the oxidant nozzle. And it is also found that the flame width becomes slightly stretched by the oxidant preheat. The peak NO mole fraction is increased by 2.026×10^{-5} with an increased NO production as the oxidant preheat temperature is increased by 200K from 300K to 500K. But CO_2 generation is not much affected by the oxidant preheat. Lim et al. (2000) suggests that such effects originates from the enhanced reaction rate of the prompt initiation reaction, $N_2+CH \rightarrow HCN+N$.

3.3.2 Effect by fuel preheat (Flame VI)

The effect by preheat of fuel mixture is studied by considering three different fuel preheat temperatures of T_F=300K, T_F=400K and T_F=500K. When the fuel inlet temperature is 500K the peak flame temperature is estimated as 1965K which is 57K higher as compared to the result obtained

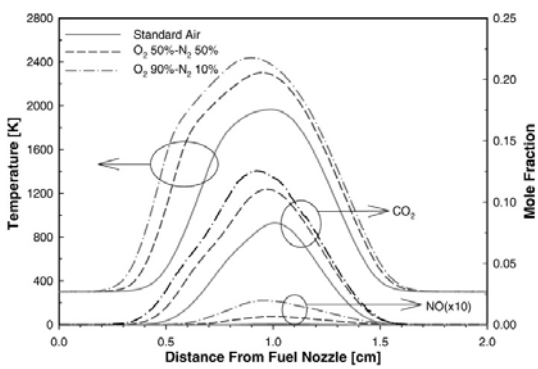

Fig. 5 Flame structure obtained for Flame IV

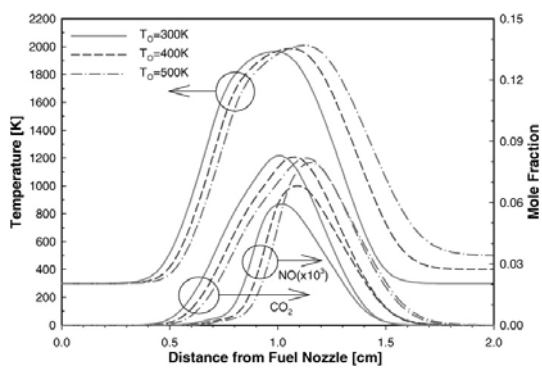

Fig. 6 Flame structure obtained for Flame V

Table 4 Results for O_2 enrichment

	Standard Air	O_2 50%	O_2 90%
Peak Temperature (K)	1965	2301	2438
Peak NO mole fraction ($\times10$)	0.000593	0.00654	0.01959
Peak CO_2 mole fraction	0.0830	0.110	0.125

Table 5 Results for Air preheat

	T_O=300K	T_O=400K	T_O=500K
Peak temperature (K)	1965	1987	2008
Peak NO mole fraction ($\times10^3$)	0.05934	0.06828	0.07960
Peak CO_2 mole fraction	0.0830	0.0824	0.0817

Table 6 Results for fuel preheat

	T_F=300K	T_F=400K	T_F=500K
Peak temperature (K)	1965	1996	2022
Peak NO mole fraction ($\times 10^3$)	0.05934	0.06723	0.07691
Peak CO_2 mole fraction	0.0830	0.0810	0.0805

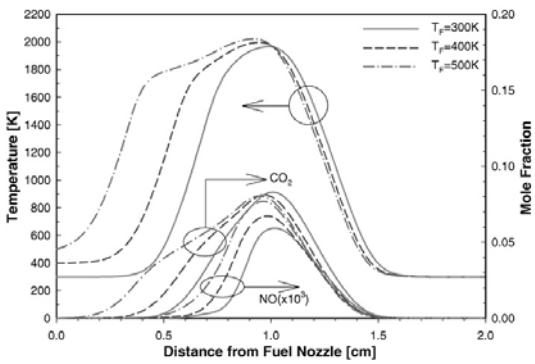

Fig. 7 Flame structure obtained for Flame VI

for T_F=300K. Figure 7 also shows that the premixed flame is shifted to the fuel nozzle and the flame width becomes significantly large as the fuel preheat temperature is increased. The peak NO mole fraction is increased by 1.757×10^{-5} as the fuel inlet temperature is increased from 300K to 500K. And we can conclude that the fuel preheat is more sensitive to the flame structure as compared to the oxidant preheat.

4. Conclusions

In this paper detailed flame structures of the CH_4/Air counterflow laminar partially premixed flames, which are formed for different inlet temperature and the introduction of additives, are studied numerically considering the nongray radiative heat transfer. The detailed chemical reactions are modeled by using the CHEMKIN-II and the OPPDIF code. The discrete ordinates method and the narrow band based WSGGM with a gray gas regrouping technique (WSGGM-RG) are applied for modeling the nongray radiative transfer. The numerical results show that the introduction of CO_2 or H_2O to the oxidant lowers the peak temperature and the NO production in flame. But O_2 enrichment causes to raise the temperature distribution and the NO production. Preheat of fuel or oxidant also causes to increase the flame temperature and the NO production. Our study shows that the fuel preheat is more sensitive than the oxidant preheat to the flame temperature and the NO production.

Acknowledgments

Authors wish to acknowledge the financial support of the CERC (Combustion Engineering Research Center).

References

Du, D. X., Axelbaum, R. L. and Law, C. K., 1991, "The Influence of Carbon Dioxide and Oxygen as Additives on Soot Formation in Diffusion Flames," *Twenty-Third Symposium (International) on Combustion*, The Combustion Institute, Pittsburgh, PA, pp. 1501~1507.

GRI MECH 2.11, http://www.me.berkeley.edu/grimech.

Goody, R. M., West, R., Chen, L. and Chrisp, D., 1989, "The Correlated-k Method for Radiation Calculations in Non-homogeneous Atmosphere," *JQSRT*, Vol. 42, No. 6, pp. 539~550.

Guo, H., Ju, Y, Maruta, K., Niioka, T. and Liu, F., 1998, "Numerical Investigation of CH/CO_2/Air and CH_4/CO_2/O_2 Counterflow Premixed Flames with Radiation Reabsorption," *Combustion Science and Technology*, Vol. 135, pp. 49~64.

Kee, R. J., Rupley, F. M. and Miller, J. A., 1989, "Chemkin-II : A FORTRAN Chemical Kinetics Package for the Analysis of Gas-phase Chemical Kinetics," *Sandia Report*, SAND89-8009.

Kim, O. J. and Song, T. H., 1996, "Implementation of the Weighted Sum of Gray Gases Model

to a Narrow band : Application and Validity," *Numerical Heat Transfer, Part B*, Vol. 30, No. 4, pp. 453～468.

Kim, O. J. and Song, T. H., 2000, "Data base of WSGGM-based Spectral Method for Radiation of Combustion Products," *JQSRT*, Vol. 64, No. 4, pp. 379～394.

Kim, O. J., Gore, J. P., Viskanta, R. and Zhu, X. L., 2003, "Prediction of Self-absorption in Opposed Flow Diffusion and Partially Premixed Flames Using a Weighted Sum of Gray Gases Model (WSGGM)-Based Spectral Model," *Numerical Heat Transfer Part A*, Vol. 44, pp. 335～353.

Kim, T. K., Menart, J. A. and Lee, H., 1991, "Nongray Radiative Gas Analyses Using the S-N Technique," *ASME Journal of Heat Transfer*, Vol. 113, pp. 946～952.

Lacis, A. A. and Oinas, V., 1991, "A Description of the Correlated k-Distribution Method for Modeling Non-gray Gaseous Absorption, Thermal Emission, and Multiple Scattering in Vertically Inhomogeneous Atmospheres," *Journal of Geophysical Research*, Vol. 96, No. D5, pp. 9027～9063.

Lee, K. Y., 2004, "The Influence of a Vortex on a Freely Propagating Laminar Methane-air Flame," *KSME International Journal*, Vol. 18, No. 5, pp. 857～864.

Li, S. C. and Williams, F. A., 1999, "NOx Formation in Two-stage Methane-air Flames," *Combustion and Flame*, Vol. 118, pp. 399～414.

Lim, J., Gore, J. and Viskanta, R., 2000, "A Study of the Effects of Air Preheat on the Structure of Methane/Air Counterflow Diffusion Flames," *Combustion and Flame*, Vol. 121, pp. 262～274.

Liu, F., Guo, H., Sallwood, G. J. and Gülder, Ö. L., 2001, "The Chemical Effects of Carbon Dioxide as an Additive in an Ethylene Diffusion Flame : Implications for Soot and NOx Formation," *Combustion and Flame*, Vol. 125, pp. 778～787.

Lutz, A. E., Kee, R. J., Grcar, J. F. and Rupley, F. M., 1997, "OPPDIF : A FORTRAN Program for Computing Opposed-flow Diffusion Flames," *Sandia Report*, SAND96-8243.

McLintock, I. S., 1968, "The Effect of Various Diluents on Soot Production in Laminar Ethylene Diffusion Flames," *Combustion and Flame*, Vol. 12, pp. 217～225.

Modest, M. F., *Radiative Heat Transfer*, McGraw-Hill, 1993.

Park, W. H. and Kim, T. K., 2003, "Application of the Weighted Sum of Gray Gases Model for Nonhomogeneous Gas Mixtures Having Arbitrary Compositions," *Proceedings of Eurotherm 73 on Computational Thermal Radiation in Participating Media*, Mons, Belgium, pp. 129～137.

Park, W. H. and Kim, T. K., 2005, "Development of the WSGGM Using a Gray Gas Regrouping Technique for the Radiative Solution within a 3-D Enclosure Filled with Nonuniform Gas Mixture," *JSME International Journal Series B*, Vol. 48, No. 2, pp. 310～311.

Soufiani, A., Taine, J., 1997, "High Temperature Gas Radiative Property Parameters of Statistical Narrow-band Model for H_2O, CO_2 and CO and Correlated- model for H_2O and CO_2," *International Journal of Heat and Mass Transfer*, Vol. 40, No. 4, pp. 987～991.

Zhu, X. L., Gore, J. P., Karpetis, A. N. and Barlow, R. S., 2003, "The Effects of Self-absorption of Radiation on an Opposed Flow Partially Premixed Flame," *Combustion and Flame*, Vol. 129, pp. 342～345.

Zhu, X. L., Takeno, T. and Core, J. P., 2002, "A Study of the Effects of Chemical Mechanism on the Computed Structure of a Radiation Sensitive Opposed Flow Partially Premixed Flame," *Combustion and Flame*, Vol. 135, pp. 351～355.